Contents lists available at ScienceDirect

BBA - Bioenergetics

journal homepage: www.elsevier.com

Photosynthetic characterization of flavodoxin-expressing tobacco plants reveals a high light acclimation-like phenotype

Rodrigo Gómez [a, 1, 2], Nicolás Figueroa [a, 1], Michael Melzer [b], Mohammad-Reza Hajirezaei [b], Néstor Carrillo [a], Anabella F. Lodeyro [a, *]

[a] Instituto de Biología Molecular y Celular de Rosario (IBR-UNR/CONICET), Facultad de Ciencias Bioquímicas y Farmacéuticas, Universidad Nacional de Rosario (UNR), 2000 Rosario, Argentina
[b] Leibniz Institute of Plant Genetics and Crop Plant Research, OT Gatersleben, Corrensstrasse 3, D-06466 Stadt Seeland, Germany

ARTICLE INFO

Keywords:
Photosynthetic electron transport chain
Plastoquinone pool
Redox state
Chloroplast
High irradiation
Flavodoxin

ABSTRACT

Flavodoxins are electron carrier flavoproteins present in bacteria and photosynthetic microorganisms which duplicate the functional properties of iron-sulphur containing ferredoxins and replace them under adverse environmental situations that lead to ferredoxin decline. When expressed in plant chloroplasts, flavodoxin complemented ferredoxin deficiency and improved tolerance to multiple sources of biotic, abiotic and xenobiotic stress. Analysis of flavodoxin-expressing plants grown under normal conditions, in which the two carriers are present, revealed phenotypic effects unrelated to ferredoxin replacement. Flavodoxin thus provided a tool to alter the chloroplast redox poise in a customized way and to investigate its consequences on plant physiology and development. We describe herein the effects exerted by the flavoprotein on the function of the photosynthetic machinery. Pigment analysis revealed significant increases in chlorophyll *a*, carotenoids and chlorophyll *a/b* ratio in flavodoxin-expressing tobacco lines. Results suggest smaller antenna size in these plants, supported by lower relative contents of light-harvesting complex proteins. Chlorophyll *a* fluorescence and P700 spectroscopy measurements indicated that transgenic plants displayed higher quantum yields for both photosystems, a more oxidized plastoquinone pool under steady-state conditions and faster plastoquinone dark oxidation after a pulse of saturating light. Many of these effects resemble the phenotypes exhibited by leaves adapted to high irradiation, a most common environmental hardship faced by plants growing in the field. The results suggest that flavodoxin-expressing plants would be better prepared to cope with this adverse situation, and concur with earlier observations reporting that hundreds of stress-responsive genes were induced in the absence of stress in these lines.

1. Introduction

Photosynthetic electron transport provides energy and reducing power for CO_2 fixation and other assimilatory pathways in plants, algae and cyanobacteria [1]. In addition, the redox status of various components of the photosynthetic electron transport chain (PETC) and the chloroplast stroma provide signals that allow the plant to adequately respond to developmental and environmental stimuli. Stress situations such as those caused by extreme temperatures, salinity and iron starvation lead to generalized inhibition of photosynthesis and down-regulation of genes encoding photosynthetic proteins including ferredoxin (Fd) [2,3]. Acceptor side limitations as those occurring during Fd decline and stress-dependent inactivation of the Calvin-Benson cycle (CBC) result in adventitious energy and electron transfer from the PETC to oxygen with increased propagation of superoxide, peroxides, singlet oxygen and other oxidants, collectively known as reactive oxygen species (ROS), which could act as signalling molecules involved in the modulation of plant stress responses and developmental programs

Abbreviations: AET, alternative electron transport; AL, actinic light; CBC, Calvin-Benson cycle; *Chl*, chlorophyll; DCMU, 3-(3,4-dichlorophenyl)-1,1-dimethylurea; DW, dry weight; Fd, ferredoxin; Fld, flavodoxin; FW, fresh weight; LHC, light-harvesting complex; MV, methyl viologen; PAR, photosynthetically active radiation; PETC, photosynthetic electron transport chain; PQ, plastoquinone; PS, photosystem; PAGE, polyacrylamide gel electrophoresis; ROS, reactive oxygen species; SDS, sodium dodecyl sulphate; WT, wild-type.

* Corresponding author.
Email address: lodeyro@ibr-conicet.gov.ar (A.F. Lodeyro)

[1] Both authors contributed equally to this study.

[2] Present address: Dipartimento di Biotecnologie, Università di Verona, Strada Le Grazie 15, 37134 Verona, Italy.

https://doi.org/10.1016/j.bbabio.2020.148211
Received 26 November 2019; Received in revised form 17 March 2020; Accepted 14 April 2020
Available online xxx
0005-2728/

[4,5]. To prevent over-reduction of the PETC in the changing environments normally found in nature, phototrophs have evolved alternative electron transport (AET) pathways that dissipate the excess of reducing power. They include cyclic electron transport, chlororespiration via alternative oxidases, and full oxygen reduction mediated by flavodiiron proteins and the Mehler-Asada cycle [6].

In cyanobacteria and some oceanic algae, the FMN-containing electron shuttle flavodoxin (Fld) is induced under various stresses as an adaptive response to the decrease of Fd at the reducing side of photosystem (PS) I [7,8]. Although they do not share any structural similarity and harbour different prosthetic groups, FMN in Fld and a 2Fe-2S cluster in Fd, the two electron carriers can be functionally exchanged in a number of enzyme-mediated oxido-reductive processes, so that Fld can replace Fd when the levels of the latter are down-regulated under most stress situations ([7] and references therein). Presumably, the main role of Fld under these conditions is to accept reducing equivalents from PSI, thus relieving the excess of excitation energy on the PETC and mitigating photo-oxidative damage and ROS propagation. Fld-encoding genes are absent from plant genomes, but introduction of a plastid-targeted cyanobacterial Fld in a number of plant species resulted in increased tolerance to multiple sources of stress, indicating that Fld could functionally interact with chloroplast oxido-reductive routes [9–15]. The plastid-located flavoprotein was able to complement Fd-deficient antisense tobacco lines [16] and decreased ROS build-up in stressed plants [12,15,17]. While Fld can be regarded as a dissipative system similar to chlororespiration, flavodiiron proteins and the Mehler-Asada pathway, a major difference does exist between them because Fld not only relieves the surplus of reducing equivalents from the PETC but also delivers them to productive chloroplast redox-based processes instead of O_2 [7].

The contribution of chloroplast redox balance to plant stress responses is extensively documented ([6] and references therein). Instead, the relationship of plastid biochemistry to leaf development has been recognized only recently [18,19]. When Fld-expressing plants are grown under normal conditions, namely, in the absence of stress, Fd and Fld accumulated to similar levels in the transgenic lines [9,20], resulting in the introduction of a new player in the network of chloroplast electron distribution. Indeed, combination of the two electron carriers did have phenotypic consequences for the corresponding plants, as reflected by higher pigment contents and photosynthetic activity per leaf cross-section [9,15,20] and delayed leaf senescence [21]. Moreover, about 1000 leaf transcripts changed their expression patterns in response to Fld presence in tobacco chloroplasts [22]. The mechanisms underlying these phenotypic effects are largely unknown. As a first step to address this question, we describe herein how chloroplast Fld affects the function of the photosynthetic machinery in plants grown under normal conditions. Measurements of chlorophyll (*Chl*) *a* fluorescence and P700 spectroscopy on wild-type (WT) and two independent tobacco lines expressing similar levels of plastid-targeted Fld revealed that the presence of the flavoprotein led to lower functional antenna size, increased PSI and PSII efficiency, higher oxidation state of the dark pool of plastoquinone (PQ) and faster PQ dark re-oxidation after a pulse of saturating light. Leaves of the transgenic lines were thicker than those of WT siblings and displayed higher *Chl a/Chl b* ratios. The collected results indicate that Fld-expressing leaves behave, in many aspects, as those found in high light-adapted plants. The consequences of this phenotype for plant survival and welfare are discussed in the light of current models of photosynthetic performance.

2. Materials and methods

2.1. Plant growth and pigment determination

Lines *pfld5-8* and *pfld4-2*, expressing Fld in plastids of tobacco plants (*Nicotiana tabacum* cv. Petit Havana) were used throughout this research together with their WT parental. Details on the design and preparation of *pfld* plants are given elsewhere [9]. Hypochlorite-sterilized seeds were germinated on half-strength Murashige-Skoog agar [23]. After 3 weeks, seedlings were transferred to soil and grown at 200 μmol photons $m^{-2} s^{-1}$ in a 16 h/8 h photoperiod and a controlled temperature of 25 °C (growth chamber conditions). The fourth fully expanded leaves of 8-weeks old plants were used for the experiments.

Chlorophylls and carotenoids were extracted from leaf sections using 96% (v/v) ethanol, and their concentrations were estimated by spectrophotometric measurements [24].

2.2. Structural analysis of leaf tissue by light microscopy

Cuttings of 2 mm^2 from the central part of the fourth fully expanded leaf from three different plants of WT, *pfld5-8* and *pfld4-2* were used to prepare samples for histological examination. Conventional and microwave-assisted fixation substitution, resin embedding, sectioning, and microscopic analysis were performed as described [25].

2.3. Determination of photosynthetic parameters

Chl a fluorescence and P700 absorption were simultaneously measured at 25 °C using a Dual-PAM-100 system (Heinz Walz, Effeltrich, Germany). In all cases, leaves were dark-adapted for 3 h in order to inactivate the CBC. After determining F_0, F_m and P_m parameters, samples were illuminated with actinic red light (AL, 650 nm), and saturating pulses (2000 μmol photons $m^{-2} s^{-1}$) were applied at the intervals indicated below. PSI and PSII photochemical response-related parameters were directly obtained from the Dual-PAM-100 software as described by Klughammer and Schreiber [26,27], Baker [28] and Kramer et al. [29].

For determination of rapid light-response curves, after initial measurements on dark-adapted leaves were completed, AL (108 μmol photons $m^{-2} s^{-1}$) was switched on for 2 min and then 30-s illumination steps were given at 108, 139, 197, 240, 284, 363, 431, 539, 644, 854, 1033, 1239, 1631 and 2100 μmol photons $m^{-2} s^{-1}$. For quasi-steady-state measurements, illumination steps were extended to 5 min each with light intensities of 108, 240, 854 and 1631 μmol photons $m^{-2} s^{-1}$, and saturating pulses were applied every minute. Measurements during early induction of photosynthesis were carried out on 133-mm^2 leaf discs previously infiltrated with either water or 1 mM methyl viologen (MV) and kept in the dark for at least 3 h. Photosynthetic induction was followed during the first min of illumination with an AL of 197 μmol photons $m^{-2} s^{-1}$ and saturating pulses were applied every 5 s.

Fluorescence measurements on light-adapted leaves were carried out directly in the growth chamber using a portable MultispeQ v1 device controlled by the PhotosynQ platform software [30], using a red AL (200 μmol photons $m^{-2} s^{-1}$) and a 500-ms saturation pulse (3000 μmol photons $m^{-2} s^{-1}$).

Net CO_2 assimilation rates (A_{CO2}) were determined using an infrared gas analyser LI-6400 (LI-COR, Lincoln, NE) at different light intensities, essentially as described by Hajirezaei et al. [31].

2.3.1. Fluorescence induction transients recording

Fluorescence induction spectra, i.e., OJIP transients, were recorded using a Dual-PAM-100 equipment in "Fast Kinetics" mode during a

320-ms red light pulse (650 nm, 2000 μmol photons $m^{-2} s^{-1}$). Fluorescence was detected with a resolution of 20 μs.

2.3.2. PQ pool redox state estimation and re-oxidation in the dark

The redox state of the PQ pool was estimated using the method described by Tóth et al. [32]. For each sample, two OJIP transients were acquired with a 10-s interval during which a complete oxidation of the PETC was achieved by applying far-red light (intensity setting 10). The proportion of reduced PQ was calculated as $(F_j - F_{jox}) / (F_m - F_{jox})$, where F_j and F_{jox} are the fluorescence values at 3 ms of the first and second transients, respectively, and F_m is the maximal fluorescence of the first transient. For estimation of the PQ pool dark re-oxidation after a saturating pulse, three OJIP transients were recorded. A first transient was obtained from dark-adapted leaves, followed by a 30-s dark period prior to acquisition of the second OJIP. Next, leaves were far-red illuminated for 10 s before the last saturating pulse. Proportion of reduced PQ was calculated using the formula described above, but with F_j values obtained from the second OJIP transient at 3 ms.

2.3.3. Functional antenna size estimations

Effective PSII antenna size was estimated using data from *Chl* fluorescence induction at low AL intensity (12 μmol photons $m^{-2} s^{-1}$). Measurements were carried out on leaf discs infiltrated with 200 μM 3-(3,4-dichlorophenyl)-1,1-dimethylurea (DCMU) in 10 mM HEPES-NaOH pH 7.4. Integrated areas above the curves were obtained from the traces after normalization between F_0 and F_m [33,34].

Effective PSI antenna size was measured on leaf discs after infiltration with 200 μM DCMU and 1 mM MV and incubation in the dark for 3 h. P700 oxidation traces were then recorded for 10 s, during which time-period samples were illuminated continuously with red AL at 24 μmol photons $m^{-2} s^{-1}$. Time courses were then normalized between zero and the maximal values, and fitted to single exponential functions. The inverse of the half-life times ($1/\tau$) was used as a relative measure of PSI antenna size [33,35].

2.4. Tricine-SDS-PAGE of thylakoid membranes

Thylakoid membranes were prepared from the fourth fully expanded leaves of 8-weeks old plants grown under chamber conditions, essentially as described by Guiamet et al. [36]. Protein complexes from the isolated membranes were resolved in 15% Tricine-SDS-PAGE [37] and visualized by Coomassie Brilliant Blue-staining. Relative quantities of proteins of interest were estimated from digitized gels by pixel densitometry using the ImageJ software (https://imagej.nih.gov/ij/).

2.5. Statistical analyses

Results are expressed as mean values ± SE. Statistical significance analyses were carried out using ANOVA followed by Tukey's HSD multiple comparison tests. In all cases, experimental data met the assumptions required for those methods. StatGraphics Centurion XVI statistical software was used for the analyses.

3. Results

3.1. Chloroplast Fld affected leaf thickness and pigment contents in plants grown under normal conditions

To evaluate the effect of chloroplast Fld on photosynthesis, we used two independent tobacco lines (*pfld5-8* and *pfld4-2*) expressing similar levels of *Anabaena* Fld targeted to plastids [9]. In line with previous reports, they contained higher *Chl a* and carotenoids and lower *Chl b* levels per leaf fresh weight (FW) (Table 1). Accordingly, the *Chl a/Chl b* ratio was enhanced in these leaves (Table 1). Microscopic analysis (Supplementary Fig. 1) showed that *pfld* leaves were ~15% thicker than WT counterparts, accompanied by slight but significant increases in FW per area without changes in water contents (Table 1).

Table 1
Expression of Fld in chloroplasts affects leaf phenotypes under normal growth conditions.

	Wild-type	*pfld*4-2	*pfld*5-8
Chl a (μg mg^{-1} FW)†	1.99 ± 0.05 (a)	2.31 ± 0.05 (b)	2.29 ± 0.05 (b)
Chl b (μg mg^{-1} FW)†	0.62 ± 0.02 (a)	0.56 ± 0.02 (b)	0.57 ± 0.02 (b)
Chl a + b (μg mg^{-1} FW)†	2.62 ± 0.05 (a)	2.86 ± 0.06 (b)	2.86 ± 0.05 (b)
Chl a/Chl b†	3.22 ± 0.09 (a)	4.08 ± 0.09 (b)	4.03 ± 0.08 (b)
Carotenoids (μg mg^{-1} FW)†	0.34 ± 0.02 (a)	0.50 ± 0.02 (b)	0.48 ± 0.02 (b)
Leaf cross-section (μm)‡	253.44 ± 1.87 (a)	285.95 ± 2.06 (b)	282.46 ± 2.18 (b)
FW/area (mg mm^{-2})†	21.81 ± 0.27 (a)	23.44 ± 0.28 (b)	23.26 ± 0.29 (b)
FW/DW†	10.50 ± 0.21 (a)	10.25 ± 0.23 (a)	10.21 ± 0.21 (a)

Results are expressed as means ± SE. Distinct letters between parentheses denote significant statistical differences between means according to Tukey's multiple comparison test ($p < 0.05$). FW, fresh weight; DW, dry weight.
† $n = 17–20$.
‡ $n = 33–45$.

3.2. Fld expression led to higher maximal PSII quantum yield and PQ oxidation state

Maximal efficiency of PSII (F_v/F_m) was measured by applying a strong saturating pulse of AL (2000 μmol photons $m^{-2} s^{-1}$) on leaves of dark-adapted tobacco plants. As shown in Fig. 1a, F_v/F_m values were significantly higher in *pfld* leaves compared to WT counterparts. Decrease of the basal fluorescence F_0 accounts for the F_v/F_m increase (Fig. 1b), without a concomitant modification of their maximal fluorescence F_m (Fig. 1c).

To further characterize the energy conversion processes at PSII reaction centres, we used fast *Chl a* fluorescence kinetics analysis (OJIP). In this technique, illumination of dark-adapted leaves with a strong light pulse (2000 μmol photons $m^{-2} s^{-1}$) causes a polyphasic fluorescence rise from the minimal level F_0 (the O level) to reach the maximal value F_m (P level) via two intermediate steps: J, reached at 2–3 ms, and I at around 30–50 ms [38]. The kinetics of this fluorescence rise is largely determined by changes in the redox state of the primary acceptor Qa and provides information about the redox state of the PETC. The O-J transient reflects the reduction of the acceptor side of PSII (Qa), whereas the J-I phase is associated with reduction of the PQ pool. The I-P rise, on the other hand, is related to the reduction of acceptors of PSI [39–41]. Fig. 2a shows raw OJIP transients obtained from attached, dark-adapted leaves of WT and *pfld* plants. An evident shift to lower values could be observed in *pfld* transients relative to WT siblings. Double normalization of OJIP values was carried out between F_0 and F_m [$Vt = (F_t - F_0) / (F_m - F_0)$] for direct comparison of fluorescence kinetics irrespective of their total amplitudes. As shown in Fig. 2b, *pfld* plants displayed a slower reduction kinetics compared to their WT counterparts. These alterations, together with the increase in *Chl a/Chl b* ratio, may reflect a reduction of the effective antenna size [42,43].

Furthermore, variations such as those observed in the J step have been associated to changes in the PQ pool redox status under dark-adapted conditions [44–48]. To test whether this was the case for *pfld* plants, we estimated the PQ pool reduction state using fast fluorescence kinetics as described by Tóth et al. [32] (see Materials and methods). Fig. 2c shows that *pfld* plants displayed a more oxidized PQ pool (~6%) when compared to WT siblings. Additionally, we monitored the re-oxidation of the PQ pool after 30 s of darkness using a sim-

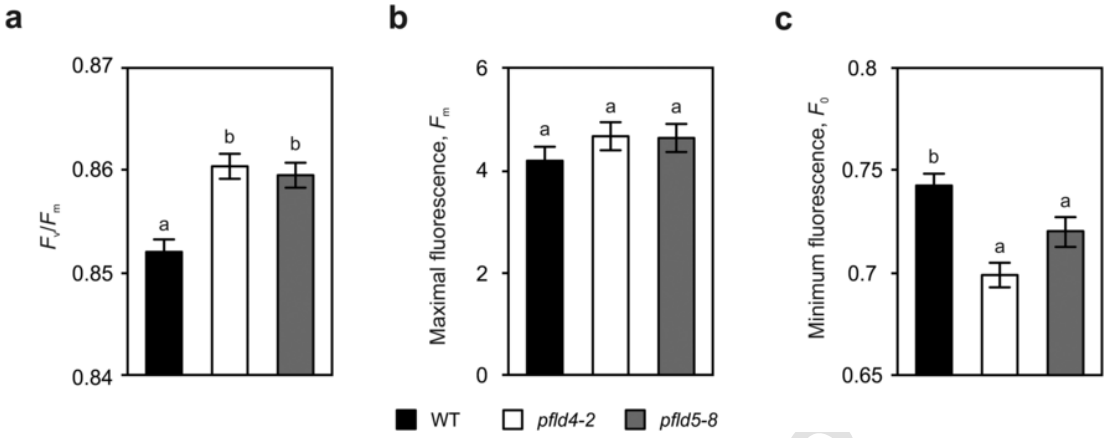

Fig. 1. Fld expression improves maximal PSII quantum yield by decreasing minimum fluorescence F_0. The F_v/F_m (a), F_m (b) and F_0 (c) parameters were obtained from *Chl a* fluorescence measurement on dark-adapted leaves of WT (black bars) and two independent transgenic lines, *pfld4-2* (white bars) and *pfld5-8* (grey bars). Results are expressed as means ± SE, $n = 24$. Different letters above the bars denote significant statistical differences between mean values estimated by ANOVA and Tukey's multiple comparison test ($p < 0.05$).

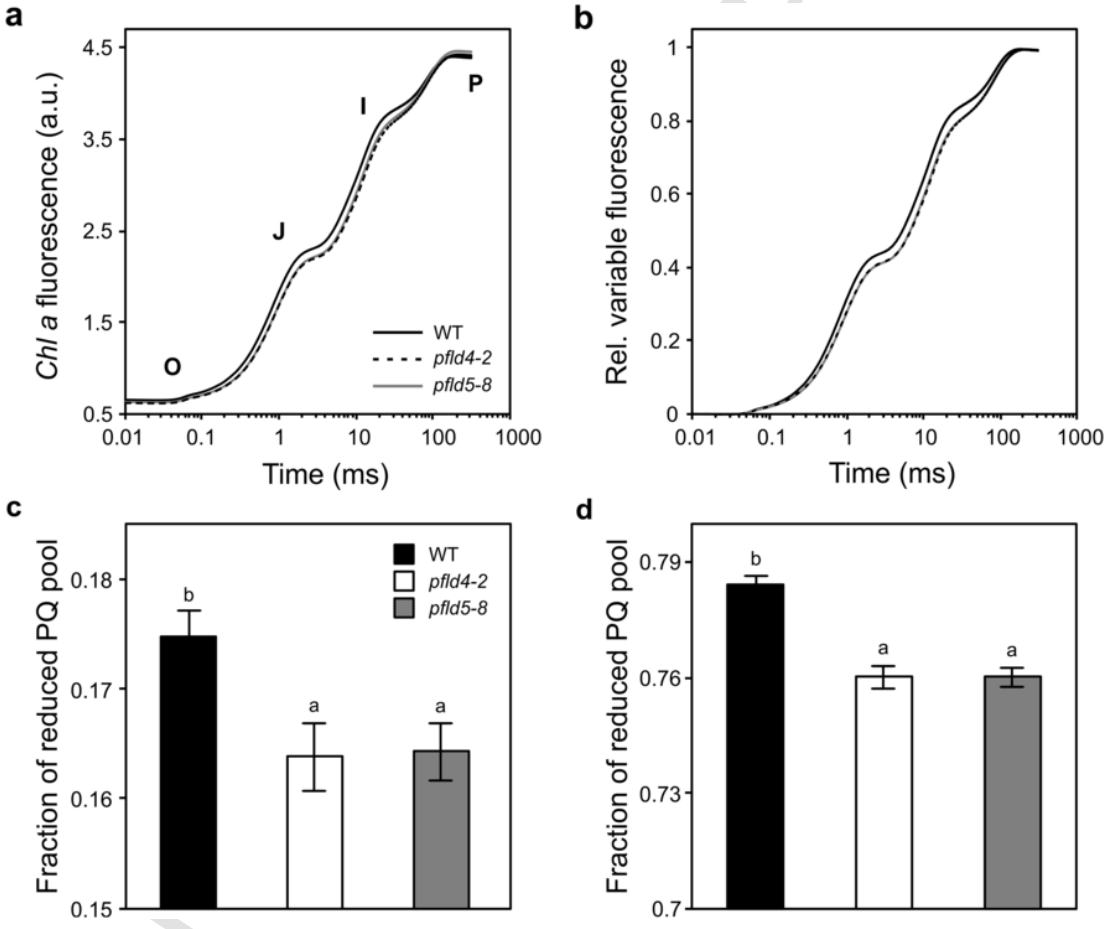

Fig. 2. Fld-expressing plants exhibit a more oxidized PQ pool and higher rates of PQ re-oxidation. Raw (a) and normalized (b) average OJIP transients ($n = 12–15$) obtained from dark-adapted leaves of WT (black solid lines), *pfld4-2* (black dashed lines) and *pfld5-8* (grey lines) tobacco plants, plotted in a logarithmic time scale. Relative normalized fluorescence was calculated as $V_t = (F_t - F_0) / (F_m - F_0)$. c) Proportion of reduced PQ, calculated as $(F_j - F_{jox}) / (F_m - F_{jox})$ from OJIP traces of dark-adapted and post far-red illuminated tobacco leaves. d) Proportion of reduced PQ after a saturating pulse of AL followed by a 30-s dark period. Results are expressed as mean values ± SE ($n = 15–18$) of WT (black bars), *pfld4-2* (white bars) and *pfld5-8* (grey bars) tobacco lines. Different letters above the bars indicate significant statistical differences between means (ANOVA and Tukey's multiple comparison test, $p < 0.05$).

ilar protocol with slight modifications (see Materials and methods). After that short period of darkness following complete reduction with a saturation pulse, PQ dark reduction was significantly lower in *pfld* plants compared to WT siblings (Fig. 2d).

3.3. Fld-expressing plants showed improved photosynthetic performance at high light intensities

To evaluate how *pfld* plants coped with different light intensities, rapid light-response curves were determined on plants grown at

200 μmol photons $m^{-2} s^{-1}$. From these measurements, an increased quantum yield of PSII (Φ_{PSII}, Fig. 3a) was observed in Fld-expressing plants relative to WT siblings, mostly at moderate to high light intensities (240 to 2100 μmol photons $m^{-2} s^{-1}$). A similar behaviour could be observed for the PSI quantum yield (Φ_{PSI}, Fig. 3b), with *pfld* plants showing greater values under high irradiation (above 539 μmol photons $m^{-2} s^{-1}$) compared to WT leaves. The oxidation state of the PQ pool, estimated by the qL parameter [29], also showed a significant increase in both transgenic lines at light intensities higher than 240 μmol photons $m^{-2} s^{-1}$ (Fig. 3c), while under the same conditions the oxidation state of PSI, quantified as Φ_{ND}, was lower in *pfld* plants (Fig. 3d). No significant differences were observed in the Φ_{NA} parameter, which describes PSI acceptor side limitation (Supplementary Fig. 2).

We also determined rapid light-response curves in an extended time-frame (up to 5 min), using a similar approach with a reduced number of steps, as adapted from Tikkanen et al. [49]. This experimental set-up allowed a closer estimation of photosynthetic parameters under quasi-steady-state conditions. Four illumination regimes were tested, corresponding to approximately 0.5-, 1-, 4- and 8-times the light intensity in the growth chamber. Results indicated that the quantum yields of both photosystems were higher in the transgenic lines at the growth light intensity and higher (Fig. 4a, b). In a similar way, the qL parameter exhibited significant increases in *plfd* plants relative to WT siblings at higher light intensities (Fig. 4c). Moreover, the oxidation state of PSI, as estimated by the Φ_{ND} parameter, exhibited significantly lower values at high light intensities (Fig. 4d). Again, no differences were observed in the Φ_{NA} parameter (Supplementary Fig. 3).

Finally, determination of Φ_{PSII} on light-adapted leaves from plants grown at 200 μmol photons $m^{-2} s^{-1}$ confirmed the results obtained under quasi-steady-state illumination conditions. Measurements were taken at midday directly in the growth chamber, in order to achieve a photosynthetic steady-state condition. Significantly higher Φ_{PSII} values ($p < 0.01$) were observed in both Fld-expressing lines (*pfld*4-2 = 0.6134 ± 0.0056; *pfld*5-8 = 0.6128 ± 0.0054) compared to WT plants (0.5902 ± 0.0044).

3.4. Photosynthetic induction during early dark-to-light transitions showed increased efficiency of both photosystems in Fld-expressing plants

We further studied the response of *pfld* plants during photosynthesis induction at the onset of illumination after long dark adaptation. Determinations were carried out using an AL intensity similar to that of the growth chamber, and saturating pulses were applied every 5 s to measure photosynthetic parameters. Leaf discs of 8-weeks old plants were infiltrated with either water (controls) or 1 mM MV, and then incu-

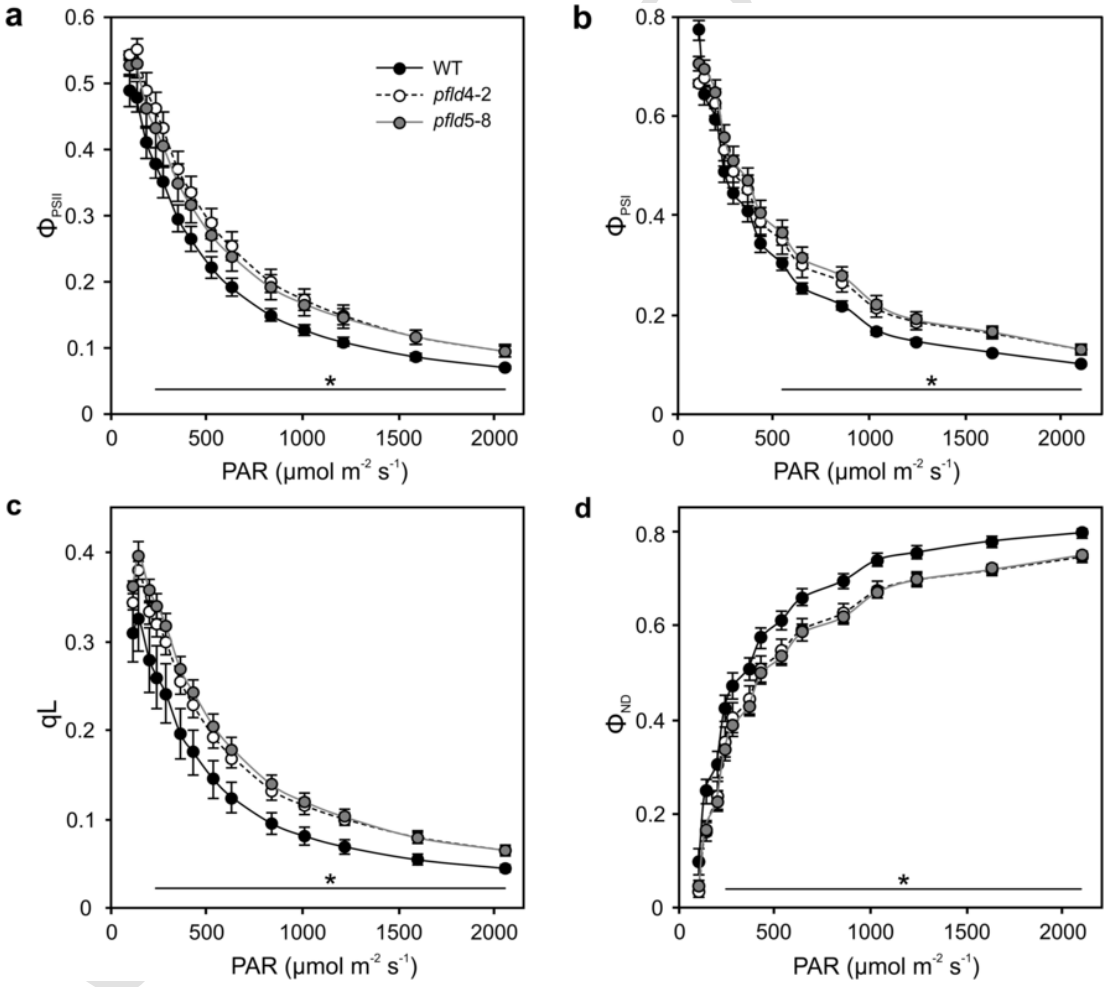

Fig. 3. Improved photosynthetic performance of *pfld* plants at high light intensities. Rapid light-response curves showing variations in Φ_{PSII} (a), Φ_{PSI} (b), qL (c) and Φ_{ND} (d) parameters as a function of PAR values from WT (black circles), *pfld4-2* (white circles) and *pfld5-8* (grey circles) plants. Illumination steps of 30 s were applied at 108, 139, 197, 240, 284, 363, 431, 539, 644, 854, 1033, 1239, 1631 and 2100 μmol photons $m^{-2} s^{-1}$. Results are expressed as means ± SE, $n = 6$–8. At each photosynthetically active radiation (PAR) assayed, genotype effects on mean differences were tested for statistical significance using ANOVA and Tukey's multiple comparison test ($p < 0.05$). Points at which statistical differences between WT and both *pfld* lines were observed are indicated with asterisks.

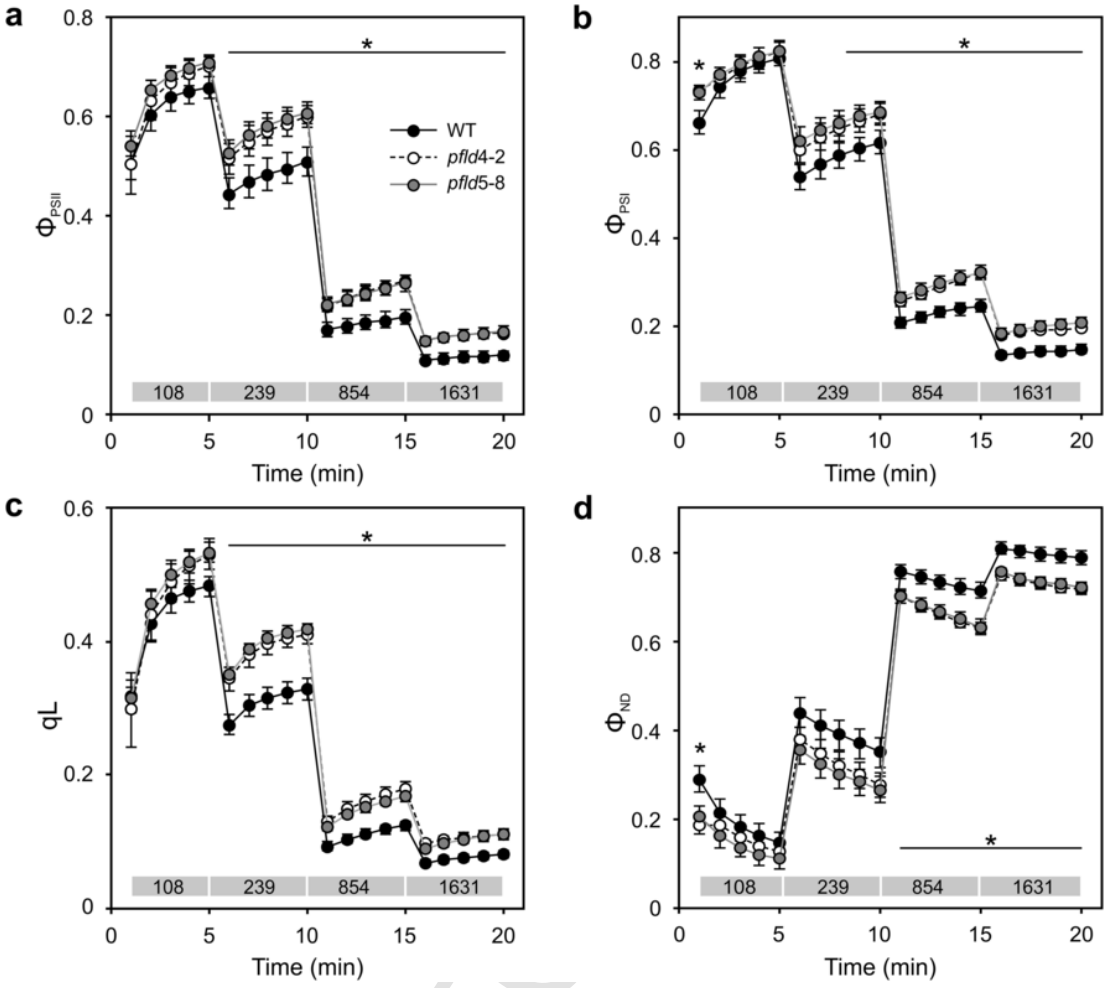

Fig. 4. Enhanced photosynthetic performance of Fld-expressing plants at moderate to high light under a quasi-steady-state regime. Extended light curves following variations in Φ_{PSII} (a), Φ_{PSI} (b), qL (c) and Φ_{ND} (d) parameters during 5-min steps of increasing illumination from WT (black circles), *pfld4-2* (white circles) and *pfld5-8* (grey circles) tobacco lines. PAR values (μmol photons $m^{-2} s^{-1}$) are indicated by grey boxes above the x-axis. Results are presented as means ± SE, $n = 6–8$. At each measuring point, statistical differences between mean values were estimated using ANOVA and Tukey's multiple comparison test ($p < 0.05$). Statistical differences between WT and both *pfld* lines are indicated with asterisks.

bated in the dark for 3 h to assure complete inactivation of the CBC. The herbicide MV is known to accept electrons directly from PSI and was used here to eliminate any acceptor side limitation on this photosystem.

In control leaf discs infiltrated with water, Φ_{PSII} and qL failed to show significant differences between lines at the beginning of illumination, but after 30 s of light exposure, *pfld* plants displayed significant increments of both parameters with respect to WT counterparts (Fig. 5a and c, respectively). The Φ_{PSI} parameter of *pfld* plants, on the other hand, progressed from lower values at the beginning of illumination to higher yields after 30 s of AL exposure (Fig. 5b). The P700 oxidation state (Φ_{ND}, Fig. 5d), started from almost null values in all lines, but *pfld* plants showed a less pronounced increase upon illumination, reaching significantly lower values than that of WT siblings at the end of the assay. This observation agrees well with results obtained from measurements at different light intensities (Figs. 3d and 4d). Concomitantly, higher acceptor-side limitation of PSI (Φ_{NA}, Fig. 5e) was evident in *pfld* plants along the entire experiment. It should be noted that during the induction period, the activity of the CBC is reported to be almost absent, causing transient over-reduction of stromal electron acceptors. To bypass this electronic jam at the acceptor side of PSI, leaf discs were treated with MV prior to the photosynthetic induction studies. This treatment provoked major modifications in all tested parameters, but with just minor differences (below statistical significance) between lines. Slight increments in Φ_{PSII} and Φ_{PSI} and a decrease in Φ_{NA} due to MV exposure were observed in *pfld* vs WT plants, without significant alterations in the redox status of the PQ pool (qL) and the P700 oxidation state (Φ_{ND}). As MV causes electrons to bypass the electron transfer step from PSI to Fd/Fld, it was expected that photosynthetic parameters would not change between lines. Thus, the small differences observed suggest that Fld-expressing plants might have subtle alterations in the structure/organization of their PETC that could extend beyond a mere difference in donor-side restriction of PSI.

The elevated Φ_{NA} values displayed by *pfld* leaves after prolonged dark adaptation (Fig. 5e) suggest that light reactions might become limiting at low irradiation intensities, resulting in delayed activation of the CBC. Indeed, light-response curves show that the differences in CO_2 assimilation rates between Fld-expressing and WT leaves diminished steadily with the light intensity (Supplementary Fig. 4a), even though *pfld* plants contained more chlorophyll per leaf cross-section [9,15,20]. When CO_2 uptake rates were expressed on a chlorophyll basis instead of leaf area to account for the changes in pigment composition, the differences between WT and *pfld* leaves were totally abolished below 100 μmol photons $m^{-2} s^{-1}$ (Supplementary Fig. 4b).

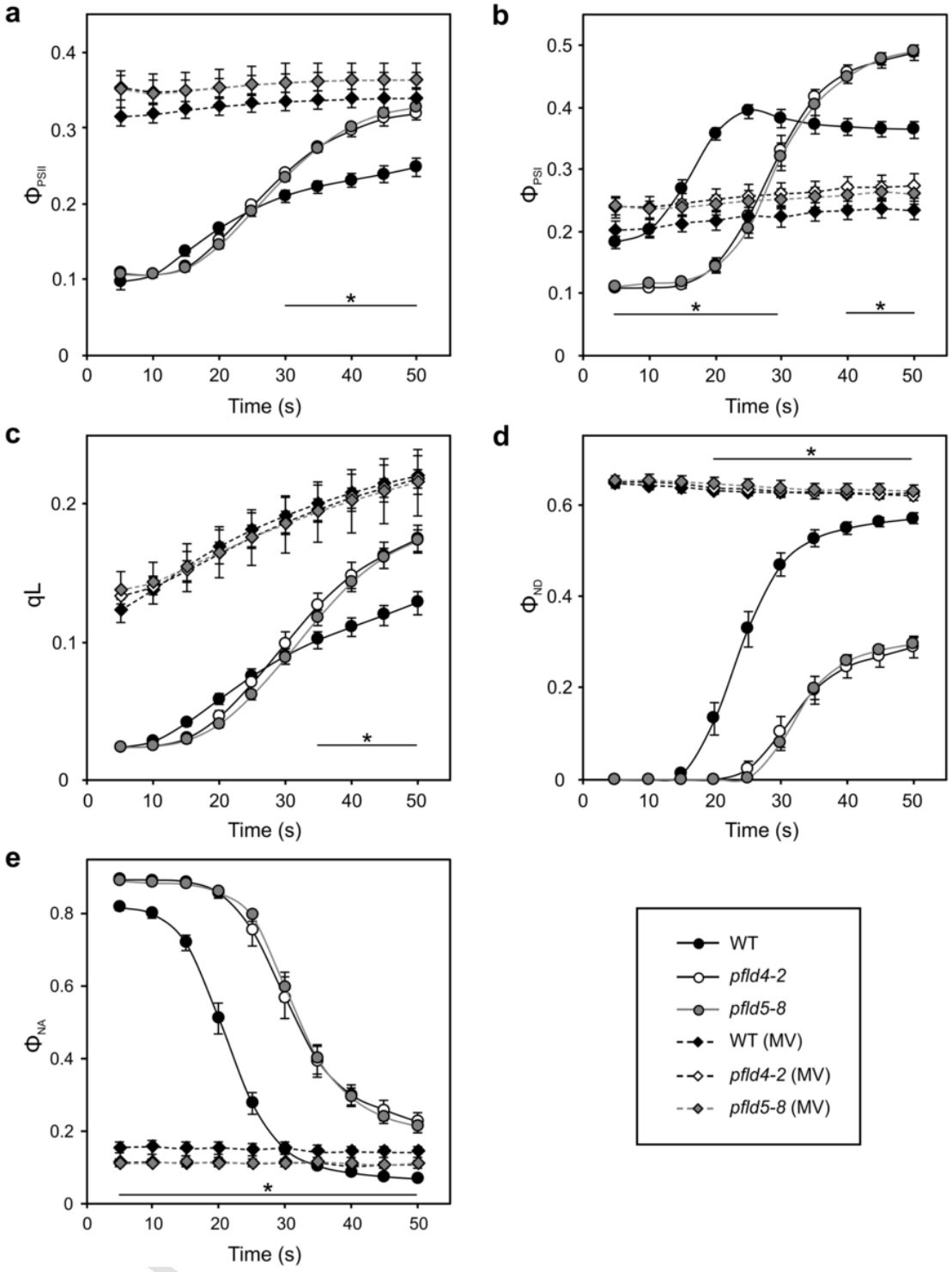

Fig. 5. Chloroplast Fld increased photosynthetic efficiency during the early period of dark-to-light transition. Photosynthetic induction curves at 240 μmol photons $m^{-2}s^{-1}$ showing Φ_{PSII} (a), Φ_{PSI} (b), qL (c), Φ_{ND} (d) and Φ_{NA} (e) parameters from dark-adapted leaf discs of WT (black symbols), *pfld4-2* (white symbols) and *pfld5-8* (grey symbols) tobacco plants. Discs were infiltrated with either water (circles, solid lines) or 1 mM MV (diamonds, dashed lines) prior to dark adaptation. Results are expressed as means ± SE, with $n = 10$. Statistical differences between mean values were determined using ANOVA and Tukey's multiple comparison tests ($p < 0.05$). For measurements from water-infiltrated leaf discs, statistical differences between WT and both *pfld* lines are indicated with asterisks. No significant differences between lines could be observed in MV-treated leaf discs.

3.5. Fld-expressing plants contained smaller functional antennae in both photosystems

Increased *Chl a/Chl b* ratios (Table 1) and downshift of the OJIP transients (Fig. 2b) in *pfld* plants suggested altered light-harvesting complex (LHC) II antennae dimensions. We further studied this effect using fast fluorescence kinetics on leaf discs poisoned with DCMU. Treatment with this agent blocks electron transfer from the Qa to Qb sites in PSII reaction centres, causing a fluorescence rise under low intensity illumination that is inversely proportional to the size of functional antennae [43]. A larger antenna would trap more radiation, causing maximal fluorescence emission to be reached faster than in reaction centres with smaller antennae. Accordingly, the area above the curve of normalized transients $(F-F_0)/(F_m-F_0)$ obtained from DCMU-treated leaf discs provides an estimation of the apparent size of LHCII [33,34]. Average transients used for calculations and mean areas are shown in Fig. 6a. From these results we confirmed that *pfld* plants exhibited a significant reduction in apparent PSII antenna size compared to their WT siblings.

The smaller size of PSII-associated antennae was also reflected in the protein composition of the corresponding thylakoid membranes, as revealed by Tricine-SDS-PAGE and protein staining (Supplementary Fig. 5a). Thylakoids isolated from Fld-expressing leaves had ~10% less Lhcb protein (normalized against the levels of the water-splitting subunit OEC33) than their WT counterparts (Supplementary Fig. 5b).

We next estimated the effective antenna size of PSI by measuring P700 oxidation on leaf discs treated with both 200 μM DCMU and 1 mM MV. DCMU was used to block PSII electron transfer to the PQ pool, and MV to avoid acceptor-side limitation on PSI. Under these donor-side limitation conditions, the rate of P700 photo-oxidation is proportional to the effective size of PSI-associated antenna [33,35]. Calculated half-time values (τ) of P700 oxidation are shown in Fig. 6b, while average transients obtained from WT and *pfld* leaf discs are given in Supplementary Fig. 6. Slower P700 photo-oxidation observed in *pfld* plants indicates a decrease in the size of functional PSI antenna compared to their WT counterparts.

4. Discussion

Plants growing in the field undergo dramatic light transitions in various time-scales that affect photosynthetic performance, development and reproduction. The dangers posed by excess of light energy and reducing power are ameliorated in the short term (seconds to minutes) through the function of dissipative systems and the regulation of the structure and function of existing thylakoid components. Additionally, long-term (hours to days) reorganization of the photosynthetic machinery via retrograde signalling to the nuclear genome favours adaptation and acclimation to the changing environment [50,51]. Acclimation, in particular, is an essential process for plant fitness as it allows them to adjust to long-term changes in environmental conditions such as light quality and intensity. It triggers a series of modifications in photosynthetic systems ranging from antenna size regulation to alterations in the expression and activity of electron sinks (such as enzymes of the CBC) to major changes in leaf morphology and physiology.

As indicated, short-term adaptive responses rely largely on dynamic regulation of light reactions and on AET pathways as main dissipative systems. Even when most of these routes generally deliver the surplus of reducing equivalents to O_2, the cyanobacterial electron carrier Fld is able to act as electron donor to a plethora of redox-based metabolic and regulatory processes. Furthermore, plants expressing chloroplast-targeted Fld displayed increased tolerance to a wide range of environmental insults [9–12]. While a large part of this protective action could be explained by replacement of isofunctional Fd under stressful conditions, combination of the two proteins in chloroplasts of plants growing under normal conditions also had phenotypic effects, such as higher photosynthetic activity and pigment contents per leaf cross-section [9,20]. We show herein that Fld presence leads to significant changes in the redox status of the PETC and in the organization of antenna components that might partly explain those previous observations.

Analysis of photosynthetic performance by measuring *Chl a* fluorescence in dark-adapted *pfld* leaves showed an increase in maximal PSII efficiency (i.e., F_v/F_m) relative to WT siblings (Fig. 1a), entirely accounted for by lower values of the minimal fluorescence F_0 (Fig. 1c). Such variation in this parameter suggests an increased PSII quenching

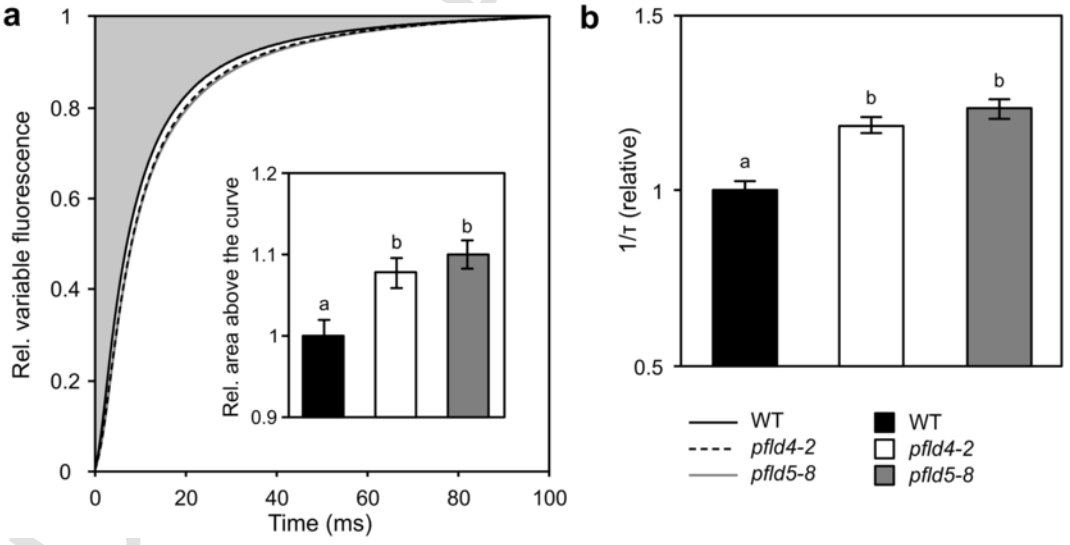

Fig. 6. Fld-expressing plants show reduced functional PSI- and PSII-associated antenna size. a) Average normalized OJIP transients recorded from WT (black solid line), *pfld4-2* (black dashed line) and *pfld5-8* (grey line) leaf discs poisoned with 200 μM DCMU and illuminated with low AL (12 μmol photons $m^{-2} s^{-1}$). The bar-plot inset shows the calculated normalized areas above the curves for WT (black bars), *pfld4-2* (white bars) and *pfld5-8* (grey bars) tobacco lines, with n = 14–18. b) Inverse of the half-life time values of normalized P700 oxidation traces obtained from tobacco leaf discs after treatment with 200 μM DCMU and 1 mM MV, and illuminated with AL of 24 μmol photons $m^{-2} s^{-1}$ (n = 12–15). In both bar plots, results are presented as means ± SE. Different letters above the bars denote statistical differences between means, according to ANOVA and Tukey's multiple comparison tests ($p < 0.05$).

capacity in *pfld* plants, which might be associated to a better packing of the PSII antenna to reaction centres [52–54] and/or changes in antenna dimensions and PS stoichiometry [42,55,56], along with factors affecting the PQ pool redox state [32].

Related to their better maximal photosynthetic efficiency, *pfld* plants also showed a more oxidized PQ pool, as estimated by OJIP analysis on dark-adapted leaves (Fig. 2c) as well as by their higher capacity to re-oxidize PQ in the dark after a saturating pulse of actinic light (Fig. 2d). In addition, when exposed to different conditions of illumination, *pfld* plants maintained a more oxidized PETC compared to WT counterparts, as reflected by their higher values of the qL parameter at moderate to high light intensities (Fig. 4c). Quantum yields of PSI and PSII were also higher in transgenic plants, but at light intensities superior to 240 μmol photons $m^{-2} s^{-1}$ (Fig. 4). Instead, the oxidation state of PSI (Φ_{ND}, Figs. 3d and 4d) was lower in *pfld* plants, with no alterations detected in the limitation on its acceptor side (Φ_{NA}, Supplementary Fig. 1). Similar trends were observed when photosynthesis induction was analysed immediately after a dark-light transition (Fig. 5). Fld-expressing plants showed higher values of Φ_{PSII} and Φ_{PSI}, and a more oxidized PQ pool, especially after 30 s of illumination (Fig. 5a, b and c, respectively). Transgenic lines also displayed a less oxidized P700 with augmented PSI acceptor-side limitation during this period (Fig. 5d and e, respectively), reflecting a slower oxidation of PSI. All these differences suggest that the organization and/or functionality of the PETC might be altered in *pfld* leaves, resembling the differences observed between low light- and high light-adapted plants [57]. During the first stages of the induction period, dark inactivation of the CBC imposes a depletion of PSI acceptors [58,59], the extension of which depends on a series of factors such as plant history and environmental pressures [60]. When this limitation was bypassed by applying MV, some differences could still be observed between WT and *pfld* lines, i.e., higher efficiency of both photosystems and lower limitation at PSI acceptor side (Fig. 5a, b, e). Those changes might reflect not only a different extent of reduction of stromal acceptors, but also alterations at the levels of thylakoid structure and/or organization. In line with that hypothesis, a decrease in the antenna size of PSII in *pfld* plants was indicated by a downshift of their OJIP transients (Fig. 2a, b) and an augmented *Chl a/Chl b* ratio, and further supported by measurements on DCMU-poisoned leaf discs (Fig. 6a) and analysis of thylakoid composition (Supplementary Fig. 5).

These observations agree well with previous results showing that Fld-expressing plants have an increased number of functional reaction centres per leaf cross-section compared to WT counterparts [15], resulting in a higher electron flow per leaf cross-section.

Taken together, the results suggest that Fld effects extend beyond a simple alteration of electron flow. Furthermore, transcriptional profiling has shown that a significant number of genes were differentially expressed in *pfld* leaves under normal growth conditions. A sub-set of them, involving hundreds of genes, were modulated in the same direction that they showed in WT siblings under stress [22]. We coined the term priming to describe those genes that display stress-like expression patterns in the absence of stress, and Fld-expressing plants have plenty of them [22]. It is worth noting, within this context, that priming has been reported to substantially contribute to the phenotypes of drought-tolerant barley varieties [61].

Interestingly enough, as shown in the present work, many of the changes introduced by Fld expression on photosynthetic performance and chloroplast biochemistry under growth (low/moderate) light conditions resemble the phenotypes displayed by high light-adapted leaves. They include increased *Chl a* and carotenoids contents per leaf FW, higher *Chl a/Chl b* ratios and electron transport rates, lower levels of PQ pool reduction and PSI oxidation, lower basal fluorescence and higher quantum efficiency of PSII/PSI operation and, prominently, reduction in antenna dimensions [25,50,51,62–74]. Leaf blade thickening as observed in *pfld* plants (Table 1 and Supplementary Fig. 1) is also a common feature of light-adapted leaves [25,71,72,75].

Light stress is likely the most common environmental hardship faced by plants growing in nature, and Fld-expressing lines display a partial high light-adapted phenotype that might help the plant to better cope with this adverse condition. Furthermore, changes in the redox poise resulting from Fld expression might trigger retrograde signals that lead to refurbishing of the photosynthetic machinery at the level of light absorption and photochemistry. It is tempting to speculate that the "light-adapted" phenotype exhibited by the transformants is part of a global response and contributes to the wide range tolerance to multiple stress sources displayed by these lines. Research is underway to test this contention and to identify Fld-primed genes that might remodel the photosynthetic machinery to more efficiently face potential environmental challenges.

Declaration of competing interest

The authors declare that they have no known competing financial interests or personal relationships that could have appeared to influence the work reported in this paper.

Acknowledgments

The authors would like to thank Mr. D. Aguirre for his technical assistance with plant growth, Felix Rose and Claudia Riemey of IPK with microscopy and Erhard Pfündel (Heinz Walz GmbH) for his valuable suggestions and help regarding the use of DUAL-PAM-100 system. R.G. and N.F. are Fellows, and N.C. and A.F.L. are Staff Members from the National Research Council (CONICET, Argentina). N.C. and A.F.L. are Faculty members of the School of Biochemical and Pharmaceutical Sciences, University of Rosario (Facultad de Ciencias Bioquímicas y Farmacéuticas, Universidad Nacional de Rosario, Argentina). This work was supported by grants PICT 2015-3828 and PICT 2017-3080 from Agencia Nacional de Promoción Científica y Tecnológica (ANPCyT, Argentina), and IO-212-17 from Agencia Santafesina de Ciencia, Tecnología e Innovación.

Appendix A. Supplementary data

Supplementary data to this article can be found online at https://doi.org/10.1016/j.bbabio.2020.148211.

References

[1] J.-D. Rochaix, Regulation of photosynthetic electron transport, Biochim. Biophys. Acta Bioenerg. 1807 (2011) 375–383, https://doi.org/10.1016/j.bbabio.2010.11.010.
[2] M.A. Gururani, J. Venkatesh, L.S.P. Tran, Regulation of photosynthesis during abiotic stress-induced photoinhibition, Mol. Plant 8 (2015) 1304–1320, https://doi.org/10.1016/j.molp.2015.05.005.
[3] P. Iovieno, P. Punzo, G. Guida, C. Mistretta, M.J. Van Oosten, R. Nurcato, H. Bostan, C. Colantuono, A. Costa, P. Bagnaresi, Transcriptomic changes drive physiological responses to progressive drought stress and rehydration in tomato, Front. Plant Sci. 7 (2016) 371, https://doi.org/10.3389/fpls.2016.00371.
[4] W. Czarnocka, S. Karpiński, Friend or foe? Reactive oxygen species production, scavenging and signaling in plant response to environmental stresses, Free Radic. Biol. Med. 122 (2018) 4–20, https://doi.org/10.1016/j.freeradbiomed.2018.01.011.
[5] G. Noctor, J.-P. Reichheld, C.H. Foyer, ROS-related redox regulation and signaling in plants, Semin. Cell Dev. Biol. 80 (2018) 3–12, https://doi.org/10.1016/j.semcdb.2017.07.013.
[6] R. Gómez, P. Vicino, N. Carrillo, A.F. Lodeyro, Manipulation of oxidative stress responses as a strategy to generate stress-tolerant crops. From damage to signaling to tolerance, Crit. Rev. Biotechnol. 39 (2019) 693–708, https://doi.org/10.1080/07388551.2019.1597829.
[7] J.J. Pierella Karlusich, A.F. Lodeyro, N. Carrillo, The long goodbye: the rise and fall of flavodoxin during plant evolution, J. Exp. Bot. 65 (2014) 5161–5178, https://doi.org/10.1093/jxb/eru273.

[8] J.J. Pierella Karlusich, R.D. Ceccoli, M. Graña, H. Romero, N. Carrillo, Environmental selection pressures related to iron utilization are involved in the loss of the flavodoxin gene from the plant genome, Genome Biol. Evol. 7 (2015) 750–767, https://doi.org/10.1093/gbe/evv031.
[9] V.B. Tognetti, J.F. Palatnik, M.F. Fillat, M. Melzer, M.-R. Hajirezaei, E.M. Valle, N. Carrillo, Functional replacement of ferredoxin by a cyanobacterial flavodoxin in tobacco confers broad-range stress tolerance, Plant Cell 18 (2006) 2035–2050, https://doi.org/10.1105/tpc.106.042424.
[10] V.B. Tognetti, M.D. Zurbriggen, E.N. Morandi, M.F. Fillat, E.M. Valle, M.-R. Hajirezaei, N. Carrillo, Enhanced plant tolerance to iron starvation by functional substitution of chloroplast ferredoxin with a bacterial flavodoxin, Proc. Natl. Acad. Sci. U. S. A. 104 (2007) 11495–11500, https://doi.org/10.1073/pnas.0704553104.
[11] M.D. Zurbriggen, V.B. Tognetti, M.F. Fillat, M.-R. Hajirezaei, E.M. Valle, N. Carrillo, Combating stress with flavodoxin: a promising route for crop improvement, Trends Biotechnol. 26 (2008) 531–537, https://doi.org/10.1016/j.tibtech.2008.07.001.
[12] M.D. Zurbriggen, N. Carrillo, V.B. Tognetti, M. Melzer, M. Peisker, B. Hause, M.-R. Hajirezaei, Chloroplast-generated reactive oxygen species play a major role in localized cell death during the non-host interaction between tobacco and Xanthomonas campestris pv. vesicatoria, Plant J. 60 (2009) 962–973, https://doi.org/10.1111/j.1365-313X.2009.04010.x.
[13] T. Coba de la Peña, F.J. Redondo, E. Manrique, M.M. Lucas, J.J. Pueyo, Nitrogen fixation persists under conditions of salt stress in transgenic Medicago truncatula plants expressing a cyanobacterial flavodoxin, Plant Biotechnol. J. 8 (2010) 954–965, https://doi.org/10.1111/j.1467-7652.2010.00519.x.
[14] Z. Li, S. Yuan, H. Jia, F. Gao, M. Zhou, N. Yuan, P. Wu, Q. Hu, D. Sun, H. Luo, Ectopic expression of a cyanobacterial flavodoxin in creeping bentgrass impacts plant development and confers broad abiotic stress tolerance, Plant Biotechnol. J. 15 (2017) 433–446, https://doi.org/10.1111/pbi.12638.
[15] F.R. Rossi, A.R. Krapp, F. Bisaro, S.J. Maiale, F.L. Pieckenstain, N. Carrillo, Reactive oxygen species generated in chloroplasts contribute to tobacco leaf infection by the necrotrophic fungus Botrytis cinerea, Plant J. 92 (2017) 761–773, https://doi.org/10.1111/tpj.13718.
[16] N.E. Blanco, R.D. Ceccoli, M.E. Segretin, H.O. Poli, I. Voss, M. Melzer, F.F. Bravo-Almonacid, R. Scheibe, M.-R. Hajirezaei, N. Carrillo, Cyanobacterial flavodoxin complements ferredoxin deficiency in knocked-down transgenic tobacco plants, Plant J. 65 (2011) 922–935, https://doi.org/10.1111/j.1365-313X.2010.04479.x.
[17] A.F. Lodeyro, N. Carrillo, Salt stress in higher plants: mechanisms of toxicity and defensive responses, in: B.N. Tripathi, M. Müller (Eds.), Stress Responses in Plants, Springer Cham, Switzerland, 2015, pp. 1–33, https://doi.org/10.1007/978-3-319-13368-3_1.
[18] M. Andriankaja, S. Dhondt, S. De Bodt, H. Vanhaeren, F. Coppens, L. De Milde, P. Mühlenbock, A. Skirycz, N. Gonzalez, G.T. Beemster, D. Inzé, Exit from proliferation during leaf development in Arabidopsis thaliana: a not-so-gradual process, Dev. Cell 22 (2012) 64–78, https://doi.org/10.1016/j.devcel.2011.11.011.0.
[19] J. Van Dingenen, L. De Milde, M. Vermeersch, K. Maleux, R. De Rycke, M. De Bruyne, V. Storme, N. Gonzalez, S. Dhondt, D. Inzé, Chloroplasts are central players in sugar-induced leaf growth, Plant Physiol. 171 (2016) 590–605, https://doi.org/10.1104/pp.15.01669.
[20] R.D. Ceccoli, N.E. Blanco, M.E. Segretin, M. Melzer, G.T. Hanke, R. Scheibe, M.-R. Hajirezaei, F.F. Bravo-Almonacid, N. Carrillo, Flavodoxin displays dose-dependent effects on photosynthesis and stress tolerance when expressed in transgenic tobacco plants, Planta 236 (2012) 1447–1458, https://doi.org/10.1007/s00425-012-1695-x.
[21] M.L. Mayta, A.F. Lodeyro, J.J. Guiamet, V.B. Tognetti, M. Melzer, M.-R. Hajirezaei, N. Carrillo, Expression of a plastid-targeted flavodoxin decreases chloroplast reactive oxygen species accumulation and delays senescence in aging tobacco leaves, Front. Plant Sci. 9 (2018) 1039, https://doi.org/10.3389/fpls.2018.01039.
[22] J.J. Pierella Karlusich, M.D. Zurbriggen, F. Shahinnia, S. Sonnewald, U. Sonnewald, S.A. Hosseini, M.-R. Hajirezaei, N. Carrillo, Chloroplast redox status modulates genome-wide plant responses during the non-host interaction of tobacco with the hemibiotrophic bacterium Xanthomonas campestris pv. vesicatoria, Front Plant Sci. 8 (2017) 1158, https://doi.org/10.3389/fpls.2017.01158.
[23] T. Murashige, F. Skoog, A revised medium for rapid growth and bio assays with tobacco tissue cultures, Physiol. Plant. 15 (1962) 473–497, https://doi.org/10.1111/j.1399-3054.1962.tb08052.x.
[24] H.K. Lichtenthaler, Chlorophylls and carotenoids: pigments of photosynthetic biomembranes, Methods Enzymol. 148 (1987) 350–382, https://doi.org/10.1016/0076-6879(87)48036-1.
[25] T. Schumann, S. Paul, M. Melzer, P. Dörmann, P. Jahns, Plant growth under natural light conditions provides highly flexible short-term acclimation properties toward high light stress, Front. Plant Sci. 8 (2017) 681, https://doi.org/10.3389/fpls.2017.00681.
[26] C. Klughammer, U. Schreiber, Complementary PS II quantum yields calculated from simple fluorescence parameters measured by PAM fluorometry and the Saturation Pulse method, PAM Appl. Notes 1 (2008) 201–247.
[27] U. Schreiber, C. Klughammer, Non-photochemical fluorescence quenching and quantum yields in PS I and PS II: analysis of heat-induced limitations using Maxi-Imaging-PAM and Dual-PAM-100, PAM Appl. Notes 1 (2008) 15–18.
[28] N.R. Baker, Chlorophyll fluorescence: a probe of photosynthesis in vivo, Annu. Rev. Plant Biol. 59 (2008) 89–113, https://doi.org/10.1146/annurev.arplant.59.032607.092759.
[29] D.M. Kramer, G. Johnson, O. Kiirats, G.E. Edwards, New fluorescence parameters for the determination of Q_A redox state and excitation energy fluxes, Photosynth. Res. 79 (2004) 209–218, https://doi.org/10.1023/B:PRES.0000015391.99477.0d.
[30] S. Kuhlgert, G. Austic, R. Zegarac, I. Osei-Bonsu, D. Hoh, M.I. Chilvers, M.G. Roth, K. Bi, D. TerAvest, P. Weebadde, MultispeQ Beta: a tool for large-scale plant phenotyping connected to the open PhotosynQ network, R. Soc. Open Sci. 3 (2016) 160592, https://doi.org/10.1098/rsos.160592.
[31] M.-R. Hajirezaei, M. Peisker, H. Tschiersch, J.F. Palatnik, E.M. Valle, N. Carrillo, U. Sonnewald, Small changes in the activity of chloroplastic $NADP^+$ dependent ferredoxin oxidoreductase lead to impaired plant growth and restrict photosynthetic activity of transgenic tobacco plants, Plant J. 29 (2002) 281–293, https://doi.org/10.1046/j.0960-7412.2001.01209.x.
[32] S.Z. Tóth, G. Schansker, R.J. Strasser, A non-invasive assay of the plastoquinone pool redox state based on the OJIP-transient, Photosynth. Res. 93 (2007) 193, https://doi.org/10.1007/s11120-007-9179-8.
[33] W.H. Wood, C. MacGregor-Chatwin, S.F. Barnett, G.E. Mayneord, X. Huang, J.K. Hobbs, C.N. Hunter, M.P. Johnson, Dynamic thylakoid stacking regulates the balance between linear and cyclic photosynthetic electron transfer, Nat. Plants 4 (2018) 116, https://doi.org/10.1038/s41477-017-0092-7.
[34] E. Belgio, E. Kapitonova, J. Chmeliov, C.D. Duffy, P. Ungerer, L. Valkunas, A.V. Ruban, Economic photoprotection in photosystem II that retains a complete light-harvesting system with slow energy traps, Nat. Commun. 5 (2014) 4433, https://doi.org/10.1038/ncomms5433.
[35] M. Ballottari, M.J. Alcocer, C. D'Andrea, D. Viola, T.K. Ahn, A. Petrozza, D. Polli, G.R. Fleming, G. Cerullo, R. Bassi, Regulation of photosystem I light harvesting by zeaxanthin, Proc. Natl. Acad. Sci. U. S. A. 111 (2014) E2431–E2438, https://doi.org/10.1073/pnas.1404377111.
[36] J. Guiamet, E. Tyystjärvi, T. Tyystjärvi, I. John, M. Kairavuo, E. Pichersky, L.D. Noodén, Photoinhibition and loss of photosystem II reaction centre proteins during senescence of soybean leaves. Enhancement of photoinhibition by the 'stay-green' mutation cytG, Physiol. Plant. 115 (2002) 468–478, https://doi.org/10.1034/j.1399-3054.2002.1150317.x.
[37] H. Schägger, G. von Jagow, Tricine-sodium dodecyl sulfate-polyacrylamide gel electrophoresis for the separation of proteins in the range from 1 to 100 kDa, Anal. Biochem. 166 (1987) 368–379, https://doi.org/10.1016/0003-2697(87)90587-2.
[38] A. Stirbet, On the relation between the Kautsky effect (chlorophyll a fluorescence induction) and photosystem II: basics and applications of the OJIP fluorescence transient, J. Photochem. Photobiol. B 104 (2011) 236–257, https://doi.org/10.1016/j.jphotobiol.2010.12.010.
[39] D. Lazár, The polyphasic chlorophyll a fluorescence rise measured under high intensity of exciting light, Funct. Plant Biol. 33 (2006) 9–30, https://doi.org/10.1071/fp05095.
[40] A. Stirbet, D. Lazár, J. Kromdijk, Chlorophyll a fluorescence induction: can just a one-second measurement be used to quantify abiotic stress responses?, Photosynthetica 56 (2018) 86–104, https://doi.org/10.1007/s11099-018-0770-3.
[41] H.M. Kalaji, G. Schansker, R.J. Ladle, V. Goltsev, K. Bosa, S.I. Allakhverdiev, M. Brestic, F. Bussotti, A. Calatayud, P. Dąbrowski, Frequently asked questions about in vivo chlorophyll fluorescence: practical issues, Photosynth. Res. 122 (2014) 121–158, https://doi.org/10.1007/s11120-014-0024-6.
[42] E. Dinç, M.G. Ceppi, S.Z. Tóth, S. Bottka, G. Schansker, The chl a fluorescence intensity is remarkably insensitive to changes in the chlorophyll content of the leaf as long as the chl a/b ratio remains unaffected, Biochim. Biophys. Acta Bioenerg. 1817 (2012) 770–779, https://doi.org/10.1016/j.bbabio.2012.02.003.
[43] S. Malkin, P.A. Armond, H.A. Mooney, D.C. Fork, Photosystem II photosynthetic unit sizes from fluorescence induction in leaves: correlation to photosynthetic capacity, Plant Physiol. 67 (1981) 570–579, https://doi.org/10.1104/pp.67.3.570.
[44] G. Schansker, A. Srivastava, R.J. Strasser, Characterization of the 820-nm transmission signal paralleling the chlorophyll a fluorescence rise (OJIP) in pea leaves, Funct. Plant Biol. 30 (2003) 785–796, https://doi.org/10.1071/fp03032.
[45] G. Schansker, S.Z. Tóth, R.J. Strasser, Methylviologen and dibromothymoquinone treatments of pea leaves reveal the role of photosystem I in the Chl a fluorescence rise OJIP, Biochim. Biophys. Acta Bioenerg. 1706 (2005) 250–261, https://doi.org/10.1016/j.bbabio.2004.11.006.
[46] S.Z. Tóth, G. Schansker, R.J. Strasser, In intact leaves, the maximum fluorescence level (FM) is independent of the redox state of the plastoquinone pool: a DCMU-inhibition study, Biochim. Biophys. Acta Bioenerg. 1708 (2005) 275–282, https://doi.org/10.1016/j.bbabio.2005.03.012.
[47] A. Stirbet, G.Y. Riznichenko, A. Rubin, Modeling chlorophyll a fluorescence transient: relation to photosynthesis, Biochemistry (Mosc) 79 (2014) 291–323, https://doi.org/10.1134/S0006297914040014.
[48] H.M. Kalaji, G. Schansker, M. Brestic, F. Bussotti, A. Calatayud, L. Ferroni, V. Goltsev, L. Guidi, A. Jajoo, P. Li, Frequently asked questions about chlorophyll fluorescence, the sequel, Photosynth. Res. 132 (2017) 13–66, https://doi.org/10.1007/s11120-016-0318-y.
[49] M. Tikkanen, S. Rantala, E.-M. Aro, Electron flow from PSII to PSI under high light is controlled by PGR5 but not by PSBS, Front. Plant Sci. 6 (2015) 521, https://doi.org/10.3389/fpls.2015.00521.
[50] M.P. Johnson, E. Wientjes, The relevance of dynamic thylakoid organisation to photosynthetic regulation, Biochim. Biophys. Acta Bioenerg. 20 (2019) 148039, https://doi.org/10.1016/j.bbabio.2019.06.011.
[51] M. Grieco, M. Tikkanen, V. Paakkarinen, S. Kangasjärvi, E.-M. Aro, Steady-state phosphorylation of light-harvesting complex II proteins preserves photosystem I under fluctuating white light, Plant Physiol. 160 (2012) 1896–1910, https://doi.org/10.1104/pp.112.206466.

[52] E. Belgio, M.P. Johnson, S. Jurić, A.V. Ruban, Higher plant photosystem II light-harvesting antenna, not the reaction center, determines the excited-state lifetime—both the maximum and the nonphotochemically quenched, Biophys. J. 102 (2012) 2761–2771, https://doi.org/10.1016/j.bpj.2012.05.004.

[53] L. Dall'Osto, S. Cazzaniga, M. Bressan, D. Paleček, K. Židek, K.K. Niyogi, G.R. Fleming, D. Zigmantas, R. Bassi, Two mechanisms for dissipation of excess light in monomeric and trimeric light-harvesting complexes, Nat. Plants 3 (2017) 17033, https://doi.org/10.1038/nplants.2017.33.

[54] A.J. Townsend, F. Saccon, V. Giovagnetti, S. Wilson, P. Ungerer, A.V. Ruban, The causes of altered chlorophyll fluorescence quenching induction in the Arabidopsis mutant lacking all minor antenna complexes, Biochim. Biophys. Acta Bioenerg. 1859 (2018) 666–675, https://doi.org/10.1016/j.bbabio.2018.03.005.

[55] M. Brestic, M. Zivcak, K. Kunderlikova, O. Sytar, H. Shao, H.M. Kalaji, S.I. Allakhverdiev, Low PSI content limits the photoprotection of PSI and PSII in early growth stages of chlorophyll b-deficient wheat mutant lines, Photosynth. Res. 125 (2015) 151–166, https://doi.org/10.1007/s11120-015-0093-1.

[56] M. Zivcak, M. Brestic, L. Botyanszka, Y.-E. Chen, S.I. Allakhverdiev, Phenotyping of isogenic chlorophyll-less bread and durum wheat mutant lines in relation to photoprotection and photosynthetic capacity, Photosynth. Res. 139 (2019) 239–251, https://doi.org/10.1007/s11120-018-0559-z.

[57] W. Huang, X. Quan, S.-B. Zhang, T. Liu, In vivo regulation of proton motive force during photosynthetic induction, Environ. Exp. Bot. 148 (2018) 109–116, https://doi.org/10.1016/j.envexpbot.2018.01.001.

[58] E. Kaiser, A. Morales, J. Harbinson, Fluctuating light takes crop photosynthesis on a rollercoaster ride, Plant Physiol. 176 (2018) 977–989, https://doi.org/10.1104/pp.17.01250.

[59] D.Y. Fan, Q. Nie, A.B. Hope, W. Hillier, B.J. Pogson, W.S. Chow, Quantification of cyclic electron flow around Photosystem I in spinach leaves during photosynthetic induction, Photosynth. Res. 94 (2007) 347–357, https://doi.org/10.1007/s11120-006-9127-z.

[60] O. Urban, M. Košvancová, M.V. Marek, H.K. Lichtenthaler, Induction of photosynthesis and importance of limitations during the induction phase in sun and shade leaves of five ecologically contrasting tree species from the temperate zone, Tree Physiol. 27 (2007) 1207–1215, https://doi.org/10.1093/treephys/27.8.1207.

[61] A. Janiak, M. Kwasniewski, M. Sowa, K. Gajek, K. Żmuda, J. Kościelniak, I. Szarejko, No time to waste: transcriptome study reveals that drought tolerance in barley may be attributed to stressed-like expression patterns that exist before the occurrence of stress, Front. Plant Sci. 8 (2018) 2212, https://doi.org/10.3389/fpls.2017.02212.

[62] S. Bailey, R.G. Walters, S. Jansson, P. Horton, Acclimation of Arabidopsis thaliana to the light environment: the existence of separate low light and high light responses, Planta 213 (2001) 794–801, https://doi.org/10.1007/s004250100556.

[63] M. Ballottari, L. Dall'Osto, T. Morosinotto, R. Bassi, Contrasting behavior of higher plant photosystem I and II antenna systems during acclimation, J. Biol. Chem. 282 (2007) 8947–8958, https://doi.org/10.1074/jbc.M606417200.

[64] W. Yamori, J.R. Evans, S. Von Caemmerer, Effects of growth and measurement light intensities on temperature dependence of CO_2 assimilation rate in tobacco leaves, Plant Cell Environ. 33 (2010) 332–343, https://doi.org/10.1111/j.1365-3040.2009.02067.x.

[65] R. Kouřil, E. Wientjes, J.B. Bultema, R. Croce, E.J. Boekema, High-light vs. low-light: effect of light acclimation on photosystem II composition and organization in Arabidopsis thaliana, Biochim. Biophys. Acta Bioenerg. 1827 (2013) 411–419, https://doi.org/10.1016/j.bbabio.2012.12.003.

[66] M. Zivcak, M. Brestic, H.M. Kalaji, Photosynthetic responses of sun- and shade-grown barley leaves to high light: is the lower PSII connectivity in shade leaves associated with protection against excess of light?, Photosynth. Res. 119 (2014) 339–354, https://doi.org/10.1007/s11120-014-9969-8.

[67] M. Zivcak, K. Brückova, O. Sytar, M. Brestic, K. Olsovska, S.I. Allakhverdiev, Lettuce flavonoids screening and phenotyping by chlorophyll fluorescence excitation ratio, Planta 245 (2017) 1215–1229, https://doi.org/10.1007/s00425-017-2676-x.

[68] R. Sato, H. Ito, A. Tanaka, Chlorophyll b degradation by chlorophyll b reductase under high-light conditions, Photosynth. Res. 126 (2015) 249–259, https://doi.org/10.1007/s11120-015-0145-6.

[69] W. Huang, Y.-J. Yang, H. Hu, S.-B. Zhang, Moderate photoinhibition of photosystem II protects photosystem I from photodamage at chilling stress in tobacco leaves, Front. Plant Sci. 7 (2016) 182, https://doi.org/10.3389/fpls.2016.00182.

[70] T. Jia, H. Ito, A. Tanaka, Simultaneous regulation of antenna size and photosystem I/II stoichiometry in Arabidopsis thaliana, Planta 244 (2016) 1041–1053, https://doi.org/10.1007/s00425-016-2568-5.

[71] S. Mathur, M.P. Sharma, A. Jajoo, Improved photosynthetic efficacy of maize (Zea mays) plants with arbuscular mycorrhizal fungi (AMF) under high temperature stress, J. Photochem. Photobiol. B 180 (2018) 149–154, https://doi.org/10.1016/j.jphotobiol.2018.02.002.

[72] M.A. Schöttler, S.Z. Tóth, Photosynthetic complex stoichiometry dynamics in higher plants: environmental acclimation and photosynthetic flux control, Front. Plant Sci. 5 (2014) 188, https://doi.org/10.3389/fpls.2014.00188.

[73] D. Takagi, S. Takumi, C. Miyake, Growth light environment changes the sensitivity of photosystem I photoinhibition depending on common wheat cultivars, Front. Plant Sci. 10 (2019) 686, https://doi.org/10.3389/fpls.2019.00686.

[74] E. Wientjes, H. van Amerongen, R. Croce, Quantum yield of charge separation in photosystem II: functional effect of changes in the antenna size upon light acclimation, J. Phys. Chem. B 117 (2013) 11200–11208, https://doi.org/10.1021/jp401663w.

[75] V.I. Mishanin, B.V. Trubitsin, M.A. Benkov, A.A. Minin, A.N. Tikhonov, Light acclimation of shade-tolerant and light-resistant Tradescantia species: induction of chlorophyll a fluorescence and P_{700} photooxidation, expression of PsbS and Lhcb1 proteins, Photosynth. Res. 130 (2016) 275–291, https://doi.org/10.1007/s11120-016-0252-z.